- Technical Paper -

FATIGUE STRENGTH AND DEFORMATION BEHAVIOR OF FLY ASH-BASED GEOPOLYMER CONCRETE

Ryojiro KATO[*1], Chikako FUJIYAMA[*2] and Januarti Jaya Ekaputri [*3]

ABSTRACT

This paper presents the fatigue strength and deformation behavior of particular fly ash-based geopolymer concrete (GP) obtained from uniaxial compressive fatigue tests with four load conditions. The number of cycle at failure of all geopolymer specimens was much shorter than that of the concrete made of the ordinary portland cement (OPC) shown in literatures. The fatigue strength for 2 million cycles of GP was lower than that of ordinary cement concrete in water and of light weight concrete. The residual axial strains and the lateral strains under cyclic load were larger than OPC when they failed.
Keywords: fly ash-based geopolymer, fatigue, elastic modulus, Poisson's ratio, maximum strain, residual strain

1. INTRODUCTION

Geopolymer concrete (GP) has been known as an eco-friendly material and as an alternative to Portland cement concrete. Specifically, effective use of fly ash for making GP is one of the strong demands in developing countries. GP are generally used for secondary products such as blocks for regaining walls and curbing. Furthermore, the mechanical properties of GP have been actively studied in decade [1][2][3]. The sleeper is one of the examples of the application of GP for the member subjected to sever external forces in Japan. In order to increase of the use of GP to structural members, further experimental studies are required. Since the mechanical properties of GP are dependent on the materials which are originally from natures instead of the well-controlled product like ordinary Portland cement (OPC).

In this study, a particular GP only from fly ash was prepared, because it is not easy to obtain blast furnace slag in some developing countries. The compressive fatigue strength and deformation behavior of this particular GP was studied. However, there are researches investigating fatigue of GP used in structural members [4][5]. The number of research relating fatigue is limited in the world.

2. TEST PROGRAMS

2.1 Materials

Material properties used in this study are shown in Table 1. Fly ash is classified as type II, and water glass is classified type 1 according to Japanese Industrial Standard (JIS). Concentration of NaOH is 8mol/L. The Polycarboxylic acid type superplasticizer is used. Density in saturated surface-dry condition of sand and gravel are 2.57 g/cm^3 and 2.67 g/cm^3 respectively. Coefficient of water absorption of sand and gravel are 2.45 % and 0.68 %, as well.

2.2 Mix proportion

Mix proportion of fly ash-based GP in this study is shown in Table 2 together with its slump flow and air. The maximum size of gravel was 20mm. The alkali to water ratio (A/W) was 0.161 where the water was used to dilute the water glass. The Silicon to Alkali ratio (Si/A) was 3.76. Superplasticizer was also used as 1.0% of fly ash. The slump flow shown here was the average value of two values measured in two orthogonal directions of a stationary sample. Cylinder specimens with 100mm of diameter and 200mm of height were casted without any difficulties due to the proper workability.

2.3 Curing condition

The curing condition is summarized in Table 3. Specimens were covered by wrap right after demolding to prevent from evaporating. Then, they were cured under 50°C for first 3 days. 50°C was the limitation temperature of our chamber for stable control. After that, they were moved into the standard condition room (temperature and humidity control room as 20°C and 60%) and put there for 25 days. Since the relative humidity was constant as 60% for both chamber and temperature condition room, specimens were always covered by wrap.

2.4 Mixing process

Mixing order and mixing time were the keys of mixing process. In this study, sands and fly ash were firstly mixed for 30 seconds. Next, the pre-mixed solution that consists of water, water glass, NaOH and superplasticizer was mixed for 60 seconds together with sand and fly ash. Gravels were divided into three portions, then subsequently mixed for 60 seconds in each.

*1 Master student, Department of Civil and Environmental Engineering, Hosei University, JCI Student Member
*2 Professor, Department of Civil and Environmental Engineering, Hosei University, JCI Member
*3 Lecturer, Institut Teknologi Sepuluh Nopember, Indonesia

Finally, additional mixing for 90 seconds was performed. To sum it up, 6 minutes were used for mixing.

2.5 Loading conditions

Loading conditions for fatigue tests were shown in Table 4. Maximum stresses level was the parameter of this study, while the minimum stress level was set as 10% of static strength. The maximum stress levels were 80%, 70%, 60% and 50% of static strength. Case "GP-S80" means the geopolymer specimen loaded from 10% to 80% cyclically. The frequency of cyclic load was always 5Hz. Experimental set up is shown in Fig.1.

The referential static strengths in accordance with the loading levels were listed in Table 5. The static strengths in Table 5 were the average values calculated from each 3 specimens which were tested in different ages to consider the increase of strengths during the fatigue test period. Case "GP-D74-S" means the geopolymer specimen tested at age 74 days with static monotonic load. It was tested after all fatigue tests.

2.6 Measurements

Applied load, axial strains (vertical strains) and lateral strains (horizontal strains) were measured by load cell and strain gauges, then simultaneously recorded with 100 Hz of sampling frequency.

To identify the decrease of stiffness due to the cyclic loads, static loading tests were performed in certain times. Elastic modulus and Poisson's ratio were calculated from stress-strain curve obtained by the static loading tests. Observations for the cracks on the surface of specimens were performed as well.

3. RESULTS AND DISUSSION

3.1 Fatigue strength

(1) Fatigue life

The number of cycles at failure of each specimen were summarized in Table 6. The average fatigue life was increased approximately 1 order when maximum stress was decreased 10%. It should be noted that the coefficient of GP-S50 was remarkably small, even those of other cases were enough small in general.

The fatigue life and the variation coefficient of ordinary cement concrete [6], ordinary cement concrete in water [7], and light weight concrete [8] are shown in Table 7. It is clear that the scatter of GP was much smaller than that of others. Furthermore, the table suggests that the fatigue life of GP tend to be smaller than that of others.

(2) S-N diagram

The relationship between stress amplitude (S) and number of cycles at failure (N) was illustrated in Fig.2. The prediction lines proposed in literatures and in JSCE standard specification [9] calculated from formula (1) were shown together.

Table1 Characteristics of materials

Mark	Name of material	Density (g/cm^3)
FA	Fly ash(type2)	2.18
WG	Water glass	1.58
NaOH	Sodium hydroxide	1.28
W	Water	1.00
S	Sands	2.57
G	Gravel	2.67
SP	superplasticizer	1.03-1.12

Table3 Curing condition

Curing Ages (days)	Normal Temperature (°C)	High Temperature (°C)	Curing Humidity (%)
28	20	50	60

Table4 Test cases

Case	Smax (%)	Smin (%)	Frequency (Hz)	Number of specimens
GP-S80	80	10	5	5
GP-S70	70			3
GP-S60	60			3
GP-S50	50			3

Table5 Results of static test

Case	Ages (days)	Static Compressive Strength (N/mm^2)	Application
GP-D31-S	31	34.7	S80,70,60
GP-D41-S	41	34.9	S50
GP-S74-S	74	37.3	-

Fig.1 Experimental set up

Table 6 Results of fatigue life

Case	Fatigue life (N)	Average (N)	Standard deviation (N)	Coefficient of variation
GP-S80	400	675	224	33.2
	508			
	600			
	865			
	1,000			
GP-S70	6,206	8,010	1,477	18.4
	7,999			
	9,824			
GP-S60	52,960	76,267	21,250	27.9
	71,496			
	104,334			
GP-S50	537,482	539,271	2,206	0.41
	537,954			
	542,379			

Table2 Mix proportions

Gmax (mm)	Slump flow (mm)	Air content (%)	A/W	Si/A	Unit mass(kg/m^3)						
					SP	WG	W	NaOH	FA	S	G
20	516.5	1.6	0.161	3.76	5.17	161	38	79	517	548	959
					283						

$$\log(N)=K\frac{(1-Smax)}{(1-Smin)} \qquad (1)$$

where Smax is the maximum stress rate and Smin is the minimum stress rate. 17 is for ordinary cement concrete, 10 is for light weight concrete or ordinary cement concrete under water for K. The S-N relationships of concrete is represented as linear when the vertical axis is maximum stress and the horizontal axis is natural logarithm of number of cycles. This can be also proved in GP tested in this study. From these results, fatigue strength for 2 million cycles of GP can be expected by the logarithmic approximation formula between fatigue life and stress of fatigue test.

Comparing the experimental results in this study and the S-N relationships calculated from standard specification, in the range of 80% to 50% of maximum stress, the experimental results were plotted between the lines using K=17 and K=10. It can be said that the fatigue life of fly ash-based GP like the specimens in this study is possibly evaluated by existing equations.

(3) Fatigue strength for 2 million cycles

S-N relationships and fatigue strength for 2 million cycles calculated from formulae obtained both experiment and literatures were shown together in Table8. Fatigue strength was expressed by the ratio of the static strength. Interestingly, fatigue strength for 2 million cycles of GP was 44.8% of its static strength. This is 24.8% lower than OPC [6], 6.4% lower than OPC in water [7] and 14.8% lower than light weight concrete [8].

3.2 Failure mode

The surface cracks of specimens of each case at the 90% of its fatigue life were shown in Fig.3. Comparing visible cracks of GP-S80 and 70 with GP-S60 and 50, the latter two cases subjected to relatively lower stresses introduced multiple surface cracks. This suggested that the micro cracks tend to be dispersed because the development of each cracks were relatively slow under the low stress level.

The specimens after the fatigue loading were shown in Fig.4. The broken specimens exhibited conical shapes for all cases. However, focusing on the height of failed specimens, there was a finding. The height of GP-S50 tended to be lower than 10cm, while that of GP-S80, 70, 60 were always higher than 10cm. Considering Figs. 2 and 3, it can be said that the process of micro-cracking inside specimens may affect

Table 7 fatigue life of cement concrete

Concrete Type	S (%)	Average of fatigue life (N)	Standard deviation (N)	CV (%)
OPC1 [6]	77	2,169(20)	2.455	113
	72	14,449(34)	29,304	203
	67	440,545(45)	960,729	218
OPC2 [7]	65	1,238(6)	1,240	105
	55	38,783(10)	21,233	54.7
	45	536,239(9)	634,433	118
LC [8]	55	74,445(11)	55,206	74.2
	52.5	425,380(5)	179,782	42.3
	50	1,382,820(10)	639,776	46.2

Note1: OPC1 is ordinary cement concrete
Note2: OPC2 is ordinary cement concrete in water
Note3: LC is Light weight concrete
Note4: Number of specimen is shown in ( )
Note5: S means the stress amplitude
Note6: CV means the coefficient of variation

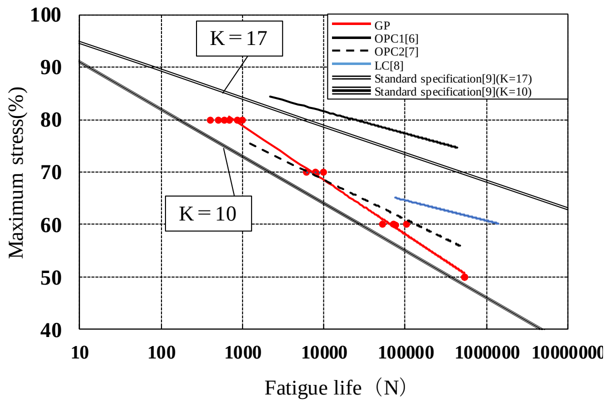

Fig.2 S-N relationships

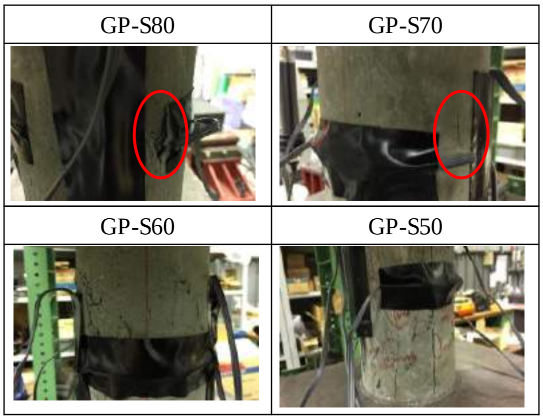

Fig.3 Cracks at the 0.9(N/Nf) of fatigue life

Table 8 S-N formula and fatigue compressive strength for 2million cycles

	Type of concrete	Smax (%)	Smin (%)	S-N formula (S= α ln(N)+ β) α	β	fatigue compressive strength (%)
GP	Geopolymer	80,70,60,50	10	-4.471	99.647	44.8
OPC1 [6]	Ordinary cement concrete	85,80,75	8	-1.832	90.474	69.5
OPC2 [7]	Ordinary cement concrete in water	75,65,55	10	-3.275	88.707	51.2
LC [8]	Light weight concrete	65,62.5,60	10	-1.69	87.122	59.6

to macro performance.

3.3 Deformation behavior

(1) Elastic modulus

The elastic modulus of GP was generally lower than that of OPC. The elastic modulus of GP obtained from static tests in this study were from 14.7 to 19.2 kN/mm^2 for 34.7 to 37.3 N/mm^2 of compressive strengths. According to standard specification [9], elastic modulus of OPC should be 28.0 and 31.0 kN/mm^2 for 30 and 40 N/mm^2 of compressive strengths, respectively.

Fig.5 shows the relationship between number of cycles and elastic modulus. The decrease rate of elastic modulus calculated from the elastic modulus obtained in the first static loading before the fatigue test shown in Fig.6 as well. Elastic modulus was calculated up to the number of cycles right before fatigue failure (shown in Table9). According to the Fig.6, in the case of GP-S80, elastic modulus right before fatigue failure was decreased to 53.5~78.7% of initial elastic modulus. In the case of GP-S70, they were 40.0~72.0% of original ones. They were 23.2~30.7% for GP-S60 and 27.5~36.6% for GP-S50. The decrease rate seems to be larger if the number of cycles at failure was longer. The decrease to 27.5~36.6% was larger than that of OPC which failed around at 2 million cycles [10].

(2) Poisson's ration

The relationship between number of cycles and Poisson's ratio was shown in Fig.7. Poisson's ratio was calculated up to the number of cycles shown in Table 9. In the case of GP-S80, Poisson's ratio right before

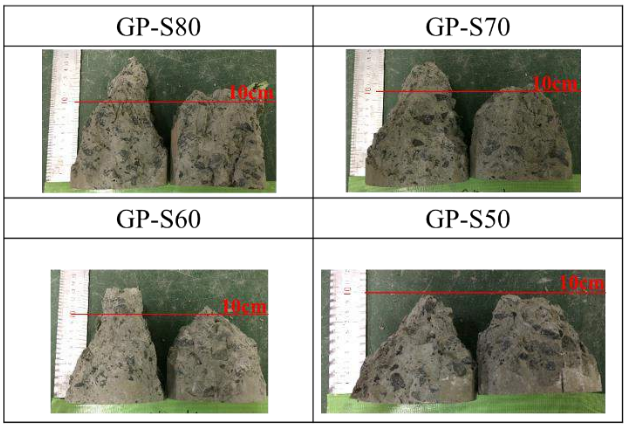

Fig.4 Failure mode

Table 9 Number of cycles right before failure

Case	Fatigue life (N)	Number of cycles right before fatigue failure (N)
GP-S80-1	400	400
GP-S80-2	600	600
GP-S80-3	865	800
GP-S80-4	1,000	1,000
GP-S70-1	6,206	6,000
GP-S70-2	7,999	7,000
GP-S70-3	9,824	9,000
GP-S60-1	52,960	50,000
GP-S60-2	71,496	70,000
GP-S60-3	104,334	100,000
GP-S50	537,482. 537,954. 542,379	500,000

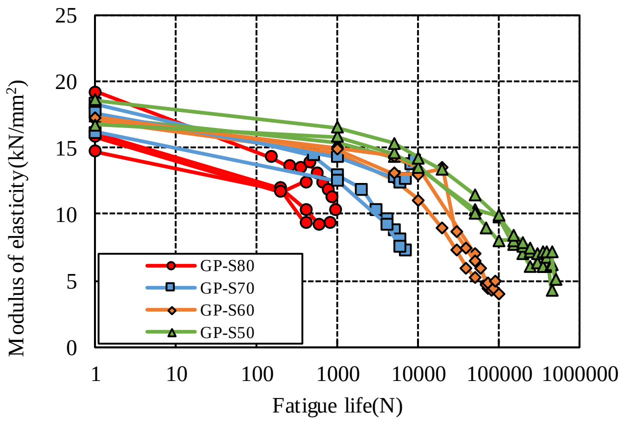

Fig.5 Modulus of elasticity and fatigue life

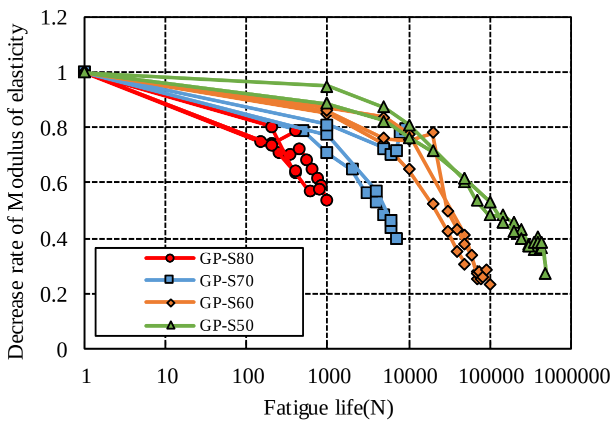

Fig.6 Decrease rate of Modulus of elasticity

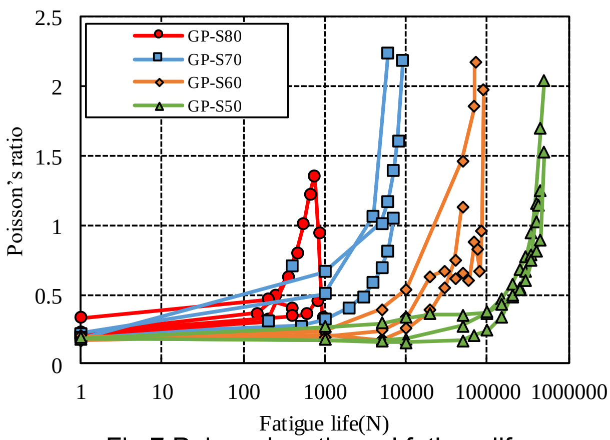

Fig.7 Poisson's ratio and fatigue life

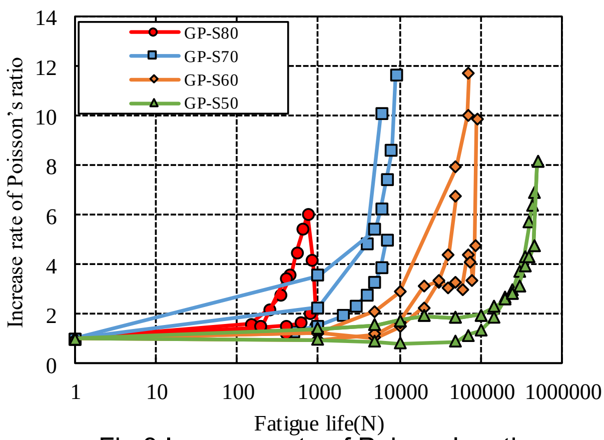

Fig.8 Increase rate of Poisson's ratio

fatigue failure were 0.34~0.71. They were 1.05~2.24 for GP-S70, 1.13~2.17 for GPS60 and 1.25~2.05 for GP-S50. Poisson's ratio of GP-S80 at ultimate state were relatively lower than that of other cases. However, there is no noteworthy tendency among GP-S70, 60, 50. The values were larger than OPC reported as about 0.5 to 1.0 [10].

Increase of the Poisson's ratio was shown in Fig.8. In the case of GP-S80, Poisson's ratios right before fatigue failure were increased to 123~602% of that before fatigue test. They were 499~1170% for GP-S70, 673~1170% for GP-S60, 694~1130% for GP-S50. Assuming the initial Poisson ratio of OPC as 0.2, the increase rate of Poisson's ratio of OPC should be 2.5~5.0.

These results indicated that the lateral deformation became dominant right before fatigue failure for GP specimens in this study.

3.3 Stress-strain curve of static loading test and fatigue test

The stress-strain curves of static loading tests and fatigue tests were demonstrated together in Fig.9. N/N_f in the figure means the number of cycles normalized by the cycle at fatigue failure. The strain up to the point where strain gages could work were shown, however the fatigue tests were continued after these records. The shapes of stress-strain curve at the beginning of cyclic load were almost linear in all cases. With the increase of the cycle, the shape of stress-strain curve became downward convex. This trend was more clearly shown in the case of lower stress levels (Fig.9 (c), (d)). This trend was probably influenced by the development of micro-cracks inside specimens shown in Fig.3.

The stress-stain curves showed us both decrease of stiffness and accumulation of residual strains. Specifically, the residual strains of GP-S60 and GP-S50 were progressively increased. Maximum residual strain in axial direction reached to -2000μ and that in lateral direction reached to 2000μ in the case of GP-S60. Those were more than -3000μ and 5000 μ for GP-S50. These values apparently exceeded the strains at failure under the static loading.

The measured maximum strains in Fig.9 were also showed a particular characteristic. The measured maximum axial strains in both directions were always larger than the strains at failure under the static loading except the axial strain of GP-S80. The maximum vertical strains of OPC failed at 245,792 to 2,120,000 cycles were -1939μ to -2980μ in literature [11]. Vertical strain of GP failed at 537,974 cycles in this study was approximately -5000μ and horizontal strain was 7000μ. This suggested that the creep of GP specimens should be examined in future.

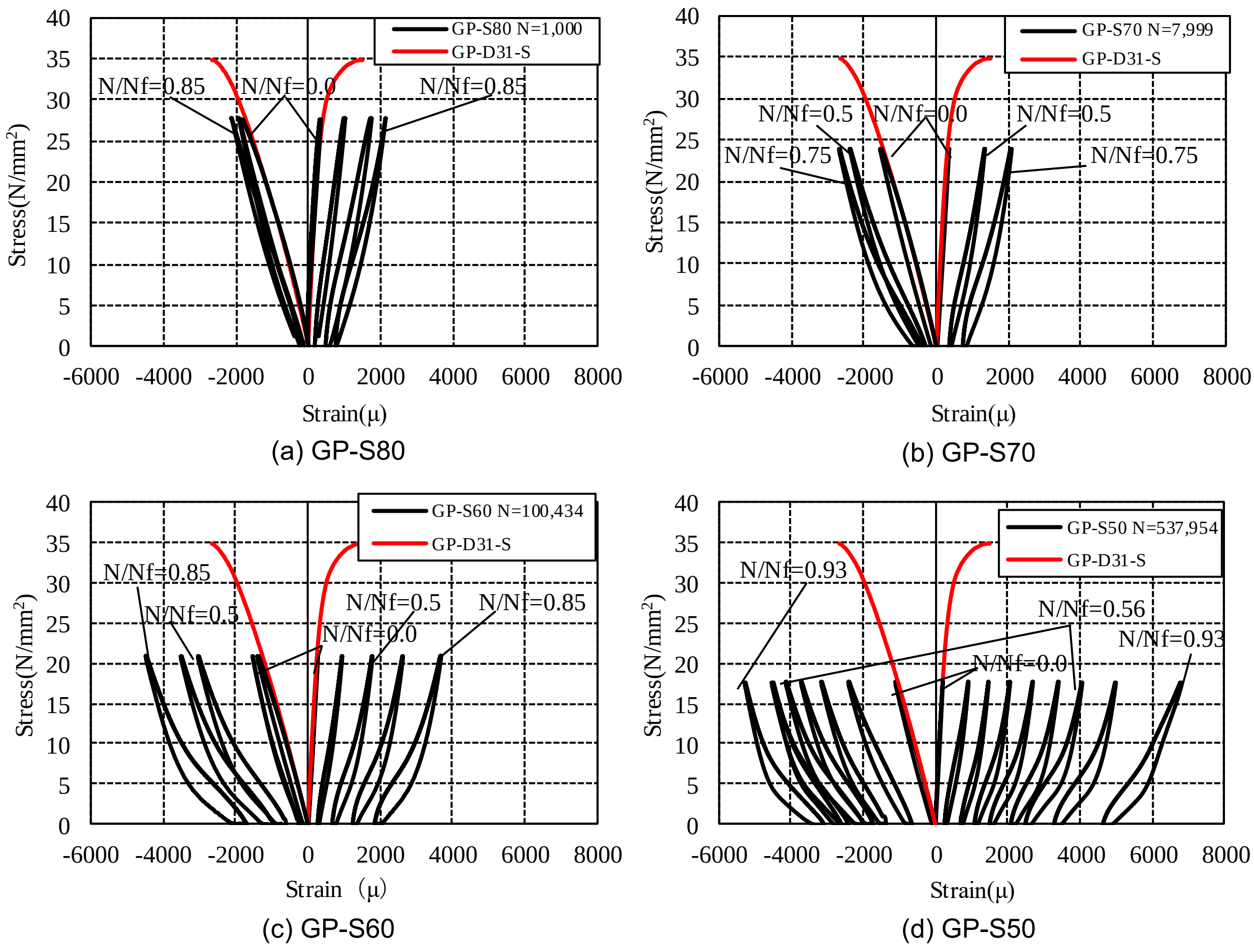

Fig.9 Stress-Strain relationships

4. CONCLUTION

The compressive fatigue tests of fly ash-based geopolymer concrete particularly prepared for this study were reported. The fatigue strength and deformation behavior were discussed by comparing preceding studies of ordinary concrete.

(1) Fatigue strength for 2 million cycles of geopolymer was about 45% of static strength. This was lower than ordinary cement concrete, ordinary cement concrete under water and light weight concrete.
(2) Elastic modulus of geopolymer concrete was originally smaller than that of ordinary Portland cement concrete. Furthermore, decrease of stiffness due to fatigue loading was larger than that of OPC.
(3) Poisson's ratio right before fatigue failure tended to be larger than that of OPC. The increase rates of Poisson's ratio were also larger than that of OPC. These results indicated that the lateral deformation became dominant right before fatigue failure of GP.
(4) The residual strains of GP-S60 and GP-S50 were progressively increased. Maximum residual strain in axial direction reached to -2000μ and that in lateral direction reached to 5000μ in the case of GP-S60. Those were more than -3000μ and 5000 μ for GP-S50. These values apparently exceeded the strains at failure under the static loading.
(5) The measured maximum axial strains in both directions were always larger than the strains at failure under the static loading except the axial strain of GP-S80. This suggested that the creep of GP specimens should be examined in future.

ACKNOWLEDGEMENT

The authors acknowledge the technical supports from the members of Institut Teknologi Sepuluh Nopember.

REFERENCES

[1] S. Ota, Y. Sagawa, K. Harada T. Nishizaki, Study on bond characteristics of reinforced bar in geopolymer mortar, Journal of japan concrete institute (JCI), Vol.38, No.1, pp2313-2318, (2016) (in Japanese)
[2] K. Minami, M. Uehara, H. Kajita, S. Funabashi, Study on compressive creep of geopolymer concrete, Journal of japan concrete institute (JCI), Vol.37, No.1, pp1894-1899, (2012) (in Japanese)
[3] H. Goda, K. Harada, K. Ichimiya, S. Tugo, K. Ikeda, Study on bending load characteristics of geopolymer concrete beams, Journal of japan concrete institute (JCI), Vol.39, No.1, pp2095-2100, (2017) (in Japanese)
[4] R. Balamuralikrishinan : Fatigue Behavior of Geopolymer Concrete, International Journal of Multidisciplinary Research and Development, Vol.2 Issue,7, pp354-359 July 2015
[5] A. Refahi, J. Aghazadeh Mohandesi, E. Gohari Behjat Abadi : Fatigue behavior of geopolymer mortar reinforced by polypropylene fibers under constant loading amplitude and variable block loading, Journal of Applied Environmental and Biological Science, 5(10S) pp477-489,2015
[6] H. Matsushita, Y. Tokumitsu, A study on compressive Fatigue strength of concrete considered survival probability. Journal of Japan Society of Civil Engineers(JSCE), Vol.284 pp127-138 (1979) (in Japanese)
[7] H. Matsushita, A study on compressive fatigue strength of concrete in the water. Journal of Japan Society of Civil Engineers(JSCE), Vol.296 pp87-95 (1980) (in Japanese)
[8] S. Hamada, M. Naruoka, An experimental study on compressive fatigue strength of light-weight concrete, Journal of Japan Society of Civil Engineers(JSCE), Vol.176 pp83-88 (1970) (in Japanese)
[9] Japan Society of Civil Engineers, Standard specifications for concrete structures-2017, design
[10] H. Matsushita, T, Makizumi, Deformation of concrete under cyclic compressive stress, Journal of japan concrete institute (JCI), Vol.1, pp77-80, (1979) (in Japanese)
[11] K. Sato, Y. Sato, Deformation behavior of concrete under repeated road, Journal of japan concrete institute (JCI), Vol.23, No,3 pp1063-1068, (2001) (in Japanese)